remote sensing

MDPI

Article

Using Multi-Temporal Landsat Images and Support Vector Machine to Assess the Changes in Agricultural Irrigated Areas in the Mogtedo Region, Burkina Faso

Farid Traoré [1,*], Joachim Bonkoungou [1], Jérôme Compaoré [1], Louis Kouadio [2], Joost Wellens [3], Eric Hallot [4] and Bernard Tychon [3]

1 Institut de l'Environnement et de Recherches Agricoles, Guisga Street, Ouagadougou, P.O. Box 8645 Ouagadougou 04, Burkina Faso; Joachbonk@gmail.com (J.B.); Jcompaore2003@yahoo.fr (J.C.)
2 Center for Applied Climate Sciences, University of Southern Queensland, West Street, Toowoomba, QLD 4350, Australia; Louis.Kouadio@usq.edu.au
3 Environmental Sciences and Management Department, University of Liege, Avenue de Longwy 185, B-6700 Arlon, Belgium; Joost.Wellens@uliege.be (J.W.); Bernard.Tychon@uliege.be (B.T.)
4 Institut Scientifique de Service Public, Rue du Chéra 200, 4000 Liège, Belgium; E.Hallot@issep.be
* Correspondence: farid.traore@yahoo.fr; Tel.: +226-25340270

Received: 16 April 2019; Accepted: 24 May 2019; Published: 18 June 2019

Abstract: Over the last few decades, small-scale irrigation has been implemented in Burkina Faso as a strategy to mitigate the impacts of adverse climate conditions. However, the development of irrigated perimeters around small and medium water reservoirs has put the water resources under significant pressure, given the uncontrolled exploitation and lack of efficacious management plan. Insights into changes in irrigated areas around these reservoirs are therefore crucial for their sustainable management while meeting the different agricultural water needs. They will help to center policy priorities in terms of major impacts on the reservoirs; and thereby elaborate relevant mitigation and/or adaptation strategies. The main objectives of this study were to (1) quantify the changes in irrigated land areas surrounding the Mogtedo water reservoir between 1987 and 2015; and (2) determine whether the irrigable potential of this reservoir could sustainably meet the agricultural water needs under a more variable and changing climate. A low-cost remote sensing method based on Landsat imagery (Thematic Mapper, Enhanced Thematic Mapper Plus, and Operational Land Imager) and using Support Vector Machine (SVM) classification was developed to detect the changes in proportion of land use/land cover (LULC) in the Mogtedo region. A forward and backward change detection analysis requiring agronomic expertise was also applied to correct the pixels temporal trajectories. In addition, an intensity analysis was performed to assess land changes at time intervals, category, and transition levels. Five main LULC classes were identified: bare and hydromorphic soils, irrigated and rainfed agricultural areas, and water bodies. Overall, the classification of LULC was satisfactory with the overall accuracy and kappa coefficients ranging from 94.22 to 95.60% and 0.92 to 0.94, respectively. Results showed that LULC transformations were faster between 2000 and 2015, compared to the 1987–2000 period. The majority of categories (LULC classes) were active in terms of intensity of change (gain or loss) during the 1987–2000 and 2000–2015 periods, except hydromorphic soils. During these periods, the transition from rainfed agricultural areas to irrigated agricultural areas were targeted and stationary. Our findings revealed a 54% increase in irrigated areas between 1987 and 2015. The reservoir water volume decreased markedly from 9,077,000 m^3 to 7,100,000 m^3 during the same period. Such a decrease threatens the satisfaction of agricultural water requirements, since the reservoir is the unique source of irrigation water in the region. It could potentially lead to conflicts between users if adequate strategies for the sustainable management of the Mogtedo reservoir are not implemented. The methodology used in this study also addressed the challenge of building up historical spatial information database in data-scarce environments, and could be replicated readily in regions or countries like Burkina Faso.

Keywords: irrigation; land use and land cover; change detection analysis; intensity analysis; Landsat; Sub-Saharan Africa

1. Introduction

Agriculture plays a crucial role in the economy of Burkina Faso, contributing to about 30% of the gross domestic product and employing over 90% of the workforce [1]. The agricultural sector faces many challenges including the year-to-year rainfall variability, poor access to irrigation water, land pressure, land tenure insecurity, expensive inputs and equipment, limited access to credit for farmers, and limited knowledge and capacity of farmers. For instance, the year-to-year rainfall variability across the Sahelian zone, including Burkina Faso, has been marked by a decrease in annual rainfall up to 40% during 1950–2000 [2–7]. In Burkina Faso, agricultural production is predominantly rainfed and farmers are typically traditional subsistence farmers. To address the negative impacts of annual rainfall variability on crop production and help farmers maintain satisfactory production over years, several governmental policy measures and programs were implemented, e.g., construction of large hydro-agricultural areas consisting of dams and irrigated perimeters in the 1970–1980s, and small-scale irrigation in the 2000s [1,8,9]. Hydro-agricultural areas more than doubled (> 60%) across the country during the 2006–2013 period, with public expenditure for irrigation infrastructure rising from 6.6 billion to 14.7 billion FCFA (about US $14 to 29 million) over 2009–2010 [1,8,10]. The development of irrigated perimeters around small and medium water reservoirs has put significant pressure on available water for irrigated agriculture, given the uncontrolled exploitation and lack of efficacious management plan and tools. Thus, a good knowledge of the water availability and proportion of irrigated land areas around the reservoir over time is crucial for a sustainable management of these irrigated areas.

Although mapping of irrigated areas is challenging due to the diverse range of irrigated plot sizes, crops, and water sources used by farmers, satellite remote sensing (RS) has emerged as an effective tool to monitor irrigated lands over a variety of climatic conditions and locations [11–14]. Satellite RS-based approaches are cost effective and less time-consuming than traditional statistical surveys. Particularly, they are valuable for monitoring irrigated land areas in developing countries, where funds are limited and few objective information is available [12]. The use of RS to identify irrigated land areas has been extensively demonstrated in various studies (see Ozdogan et al. [12] for a review). For example, Gumma et al. [13] separated irrigated and non-irrigated areas for the whole land area in Ghana using Landsat Enhanced Thematic Mapper Plus (ETM+) and MODIS 250 m data. The classification of land use/land cover (LULC) was performed using unsupervised ISOCLASS clustering K-means and decision-tree algorithms [13]. Similarly, Zoungrana et al. [15] and Knauer et al. [16] used multi-date or multi-temporal Landsat and MODIS images for the detection of changes in LULC (including agricultural lands and irrigated areas) for regions in southwest Burkina Faso in the former study, and for entire Burkina Faso in the latter. In both studies, the classification was carried out using random forest classification approach [15,16]. Traoré et al. [17] used a different classification technique (i.e., maximum likelihood classifier, MLC) with Landsat imagery and aerial photographs to assess the evolution over time of the irrigated areas in the Kou watershed, Burkina Faso. In this latter study, the authors pointed out the need for a methodology to better assess the changes in rural irrigated areas over time based on historical RS images for regions with scarce historical LULC, and thus improve the overall management of irrigated areas in the country.

Although support vector machine (SVM) has been used successfully for LULC classification in various regions worldwide (e.g., [18–20]), it has been applied in study regions in Burkina Faso for mapping soil properties [21] or urban development patterns [22], and has yet to be investigated for monitoring irrigated areas. The aims of this study were to (1) assess the changes in irrigated agricultural areas around the Mogtedo water reservoir in Burkina Faso between 1987 and 2015 using Landsat imagery and SVM classification, and (2) determine whether the irrigable potential of this reservoir

could sustainably meet the agricultural water needs under a more variable and changing climate. The findings of this study would help to improve the monitoring of irrigated agricultural areas across the Mogtedo region and center policy priorities in terms of major impacts on the reservoir, and thereby elaborate relevant mitigation and/or adaptation strategies.

2. Study Area

The Mogtedo water reservoir is located 85 km east of Ouagadougou, Burkina Faso, in the Plateau Central administrative district (Figure 1). There are three localities around the Mogtedo reservoir: Talembika and Zam in the municipality of Zam and Mogtedo in the municipality of Mogtedo. Vertisols are the dominant soil types in areas around the reservoir (Figure 1). The climate in the Mogtedo region is characterized by two seasons: a dry season from October to May, and a wet or monsoon season from June to September [23–25]. The average annual rainfall is about 800 mm and varies between 600 and 1100 mm [26,27]. Like the majority of Sahelian regions, there is a decreasing trend in annual rainfall across the Mogtedo region, clearly noticeable during the 1950–1990 period (Figure 2).

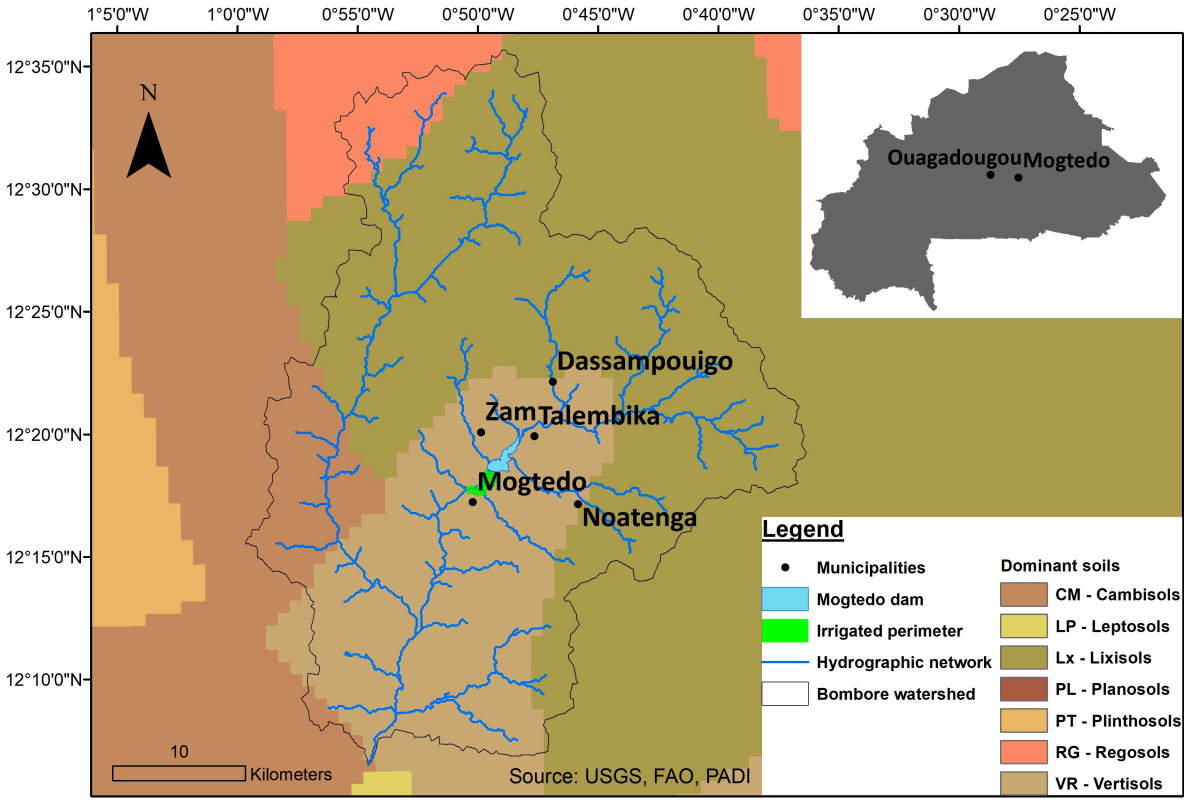

Figure 1. Map showing the Mogtedo water reservoir along with the surrounding municipalities.

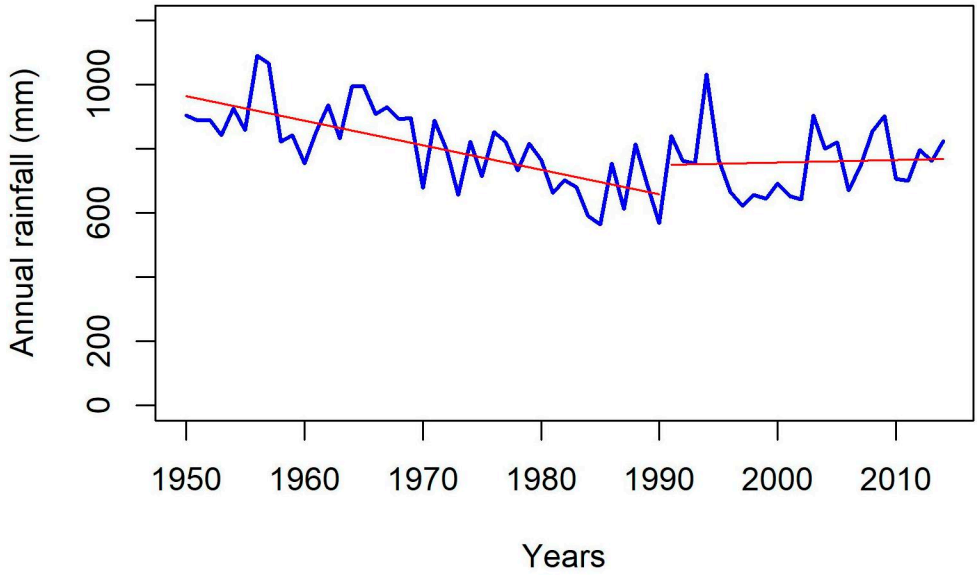

Figure 2. Annual rainfall in the Mogtedo region during 1950–2014. Trend lines for the periods 1950–1990 and 1990–2014 are shown.

The Mogtedo water reservoir was built in 1963 through programs funded by the *Fonds Européen de Développement* (FED) and the *Fonds d'Aide à la Coopération* (FAC). The reservoir is the main source of water for socio-economic activities of populations in Zam and Mogtedo municipalities [25]. The main watercourse of the study area is the Bomboré, a tributary of the Nakanbé watercourse (Figure 1). The estimated water volume in the Mogtedo reservoir varies from study to study. Ndanga Kouali [28] estimated the volume at 4,657,000 m^3, whereas Guyon et al. [29] estimated it at 7,100,000 m^3. The latter estimate was based on a Differential Global Positioning System (DGPS) topography and bathymetry with more than 2,000 measurement points, and will be used in our next analyses.

Irrigation is the predominant water use around the Mogtedo reservoir. The irrigated perimeter was built downstream of the reservoir in 1967 and consisted of a formal development of 123 ha of farms [30]. Although the number of farmers in the perimeter varies between 400–500 [26], the total number could be the double if smallholders farms outside the perimeter who also rely on the water reservoir are counted.

3. Materials and Methods

To assess the changes in irrigated agricultural areas around the Mogtedo reservoir, Landsat images from three different sensors were used: Landsat-5 TM, Landsat-7 ETM+ and Landsat-8 OLI (Table 1). They were sourced from the United States Geological Survey (USGS) website (https://earthexplorer.usgs.gov/). Images taken between January and February were considered in the study because this period corresponds to predominant irrigation activities in the study area. The study area delineated on Landsat images has 159,201 pixels.

Table 1. Landsat images used for mapping irrigated areas in the Mogtedo region, Burkina Faso.

Images	Acquisition Date	Path	Row	Spatial Resolution (m)	Bands Used
Landsat-5 TM	15 February 1987	194	52	30	1, 2, 3, 4, 5, 7
Landsat-7 ETM+	11 February 2000	194	52	30	1, 2, 3, 4, 5, 7
Landsat-8 OLI	27 January 2015	194	52	30	2, 3, 4, 5, 6, 7

The methodology used to classify the LULC classes across the Mogtedo region included the following steps (Figure 3).

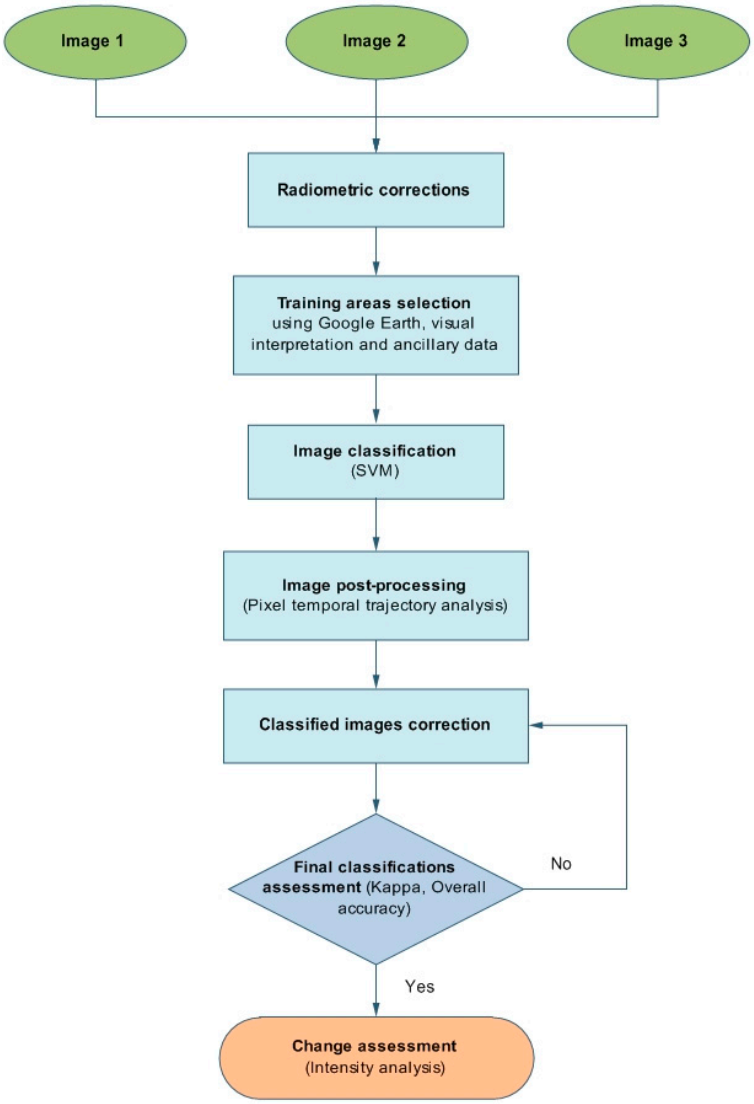

Figure 3. Flowchart of the data inputs, key procedures and data processing for mapping irrigated areas in the Mogtedo region, Burkina Faso.

3.1. Radiometric Corrections

Radiometric corrections were carried out to attenuate the atmospheric effects and provide a basis for standardized comparison of data from images acquired on different dates or by different sensors [31]. The conversions were performed following Chander and Markham [32] and Chander et al. [33].

3.2. Selection of Training and Validation Areas

Five main LULC classes were identified across the study area: bare soils, hydromorphic soils, irrigated areas, agricultural rainfed areas, and water bodies. The total number of training and validation samples varied according to LULC class and Landsat image. The number of pixel samples for irrigated areas ranged from 382 (Landsat TM) to 570 (Landsat ETM+ and OLI). That of rainfed areas and water bodies were 656 and 246, respectively, regardless of the Landsat image (Table S1). The final reference dataset for training and validation contained 3030 pixels for the year 1987, and 3204 pixels for each of the years 2000 and 2015. We used two-thirds of the sample for training and the remaining one-third for validation.

On the 1987 Landsat image, pixel samples were selected based on visual interpretations and historical data provided by farmers and local authorities. The historical data were collected through a survey involving more than 400 stakeholders. Details of the survey methodology can be found in Wellens [34]. The assessment of historical LULC was limited by the lack of ground truth information for past years. On the 2000 and 2015 Landsat images, the selection of pixel samples was carried out using Google Earth high resolution imagery. Spatially homogenous known areas of the respective LULC class were delineated by a polygon and the class was identified.

A separability analysis of LULC classes using the Jeffries-Matusita index [35] showed a separability ranging from 1.3 to 2.0.

3.3. Support Vector Machine Classification

The SVM classification method is a supervised non-parametric statistical learning technique [36–38]. SVMs have gained prominence because they are robust and can handle relatively small datasets [38,39]. A comprehensive theoretical description of SVMs is provided in Vapnik [38] and Huang et al. [40]. In our study, the default 'radial basis function' kernel was used for the SVM classifier.

Additionally, a comparison between the SVM and the Maximum Likelihood Classifier (MLC) techniques was carried out to evaluate the classification performance.

Errors in LULC classification occur generally because of noises induced by similarities in the spectral responses of some types of plant cover [41]. The quality of LULC classifications was assessed using the overall accuracy (OA) and kappa coefficient [42–45].

3.4. Images Post-Processing and Final Classification Assessment

A post-processing step was carried out through a pixel trajectory analysis to detect and correct the changes occurring in each pixel over time. Given the significant development of agriculture (irrigated and rainfed) in the study region, it would be unlikely to see a transition from cultivated farmland to bare soil. The definitive inclusion of a given pixel into a LULC class was controlled using rules based on the observed trends of this respective LULC over time. Thus, all unlikely trajectories for a given classified pixel were corrected using these rules. The RS images were then reclassified, and the classification reassessed using the same training and validation areas as defined in Section 3.2.

3.5. Change Assessment

An intensity analysis was performed to assess the changes in LULC classes between 1987, 2000, and 2015 [46,47]. This method has been used extensively to understand LULC changes (e.g., [48–52]). We used the approach proposed by [53] which can identify whether the pattern of a LULC class is stable across time intervals in terms of the intensity of gains and losses. Readers are referred to [53] and Koglo et al. [50] for a full description of the method.

RS images were processed using the Harris Geospatial Solutions™ ENVI® program and ESRI™ ArcGIS® Desktop suite. LULC classification and intensity analyses were performed using the R Language and Environment for Statistical Computing [54].

4. Results and Discussion

4.1. Accuracy Assessment before Pixel Trajectory Corrections

The OA of the three Landsat images were ≥ 88%, with the highest OA obtained for the 2015 image (Table 2). All the kappa coefficients were excellent based on the recommendations of Landis and Koch [45] and Streiner and Norman [55]. They ranged from 0.84 to 0.97 (Table 2).

Table 2. Accuracy assessment before pixel trajectory corrections.

Images	Overall Accuracy (%)	Kappa Coefficient	Agreement *
Landsat-5 TM	88.48	0.84	Excellent
Landsat-7 ETM+	90.98	0.87	Excellent
Landsat-8 OLI	95.26	0.94	Excellent

* According to Landis and Koch [45] and Streiner and Norman [55].

The detailed accuracies for each of the LULC classes in the study area are provided in Table 3. The overall user accuracy was high and ranged from 78% to 100%. The confusion between LULC classes on all three Landsat images varied according to the class and the image. For the 1987 image (Landsat 5 TM), confusions were noticeable between hydromorphic and bare soils (16.33% hydromorphic soils classified as bare soils) and between rainfed areas and bare soils (13.11% rainfed areas classified as bare soils). Such confusions can be related to the lack of historical ground truth data (i.e., surveys, inventories, or testimonies of local people) to assess the sampling of LULC classes. For the 2015 Landsat image the confusions between hydromorphic and bare soils or rainfed areas and bare soils were reduced (Table 3). Distinctions between irrigated areas and rainfed areas were clear, with the confusion between these two classes being < 1%, regardless of the image. The results of this first LULC classification are depicted in Figure 4. There was an increase in proportion of irrigated agricultural areas during the study period. Bare soils and agricultural rainfed areas around the reservoir were converted into agricultural irrigated areas between 1987 and 2015. The reservoir area also decreased between the same period (Figure 4A,C). Regarding the misclassifications, an example is shown on the 1987 Landsat image with the 'presence' of irrigated agricultural areas across the southeastern parts of the reservoir, which was anomalous (see red circle on Figure 4A).

Table 3. Classification accuracy (expressed in %) before pixel trajectory corrections for each of the LULC classes in the Mogtedo region, Burkina Faso.

	Bare Soil	Hydromorphic Soil	Irrigated Areas	Rainfed Areas	Water Bodies	User Accuracy
			Landsat 5 TM			
Bare soil	**90.73**	16.33	0.52	13.11	0	88.88
Hydromorphic soil	3.71	**73.87**	1.57	3.66	0	78.61
Irrigated areas	0.07	2.01	**97.38**	0	0	97.64
Rainfed areas	5.49	7.54	0.52	**83.23**	0	83.74
Water bodies	0	0.25	0	0	**100**	99.6
			Landsat 7 ETM+			
Bare soil	**91.25**	9.64	0.53	13.26	0	90.64
Hydromorphic soil	2.3	**84.64**	2.11	0.61	0	87.37
Irrigated areas	0	1.82	**96.49**	0.15	0	98.57
Rainfed areas	6.45	3.39	0.88	**85.98**	0	84.3
Water bodies	0	0.52	0	0	**100**	99.19
			Landsat-8 OLI			
Bare soil	**95.4**	2.6	0	3.2	0	97.65
Hydromorphic soil	1.34	**90.36**	2.81	2.13	0	87.85
Irrigated areas	0.07	3.65	**97.19**	0.3	0	97.02
Rainfed areas	3.19	3.39	0	**94.36**	0	91.7
Water bodies	0	0	0	0	**100**	100

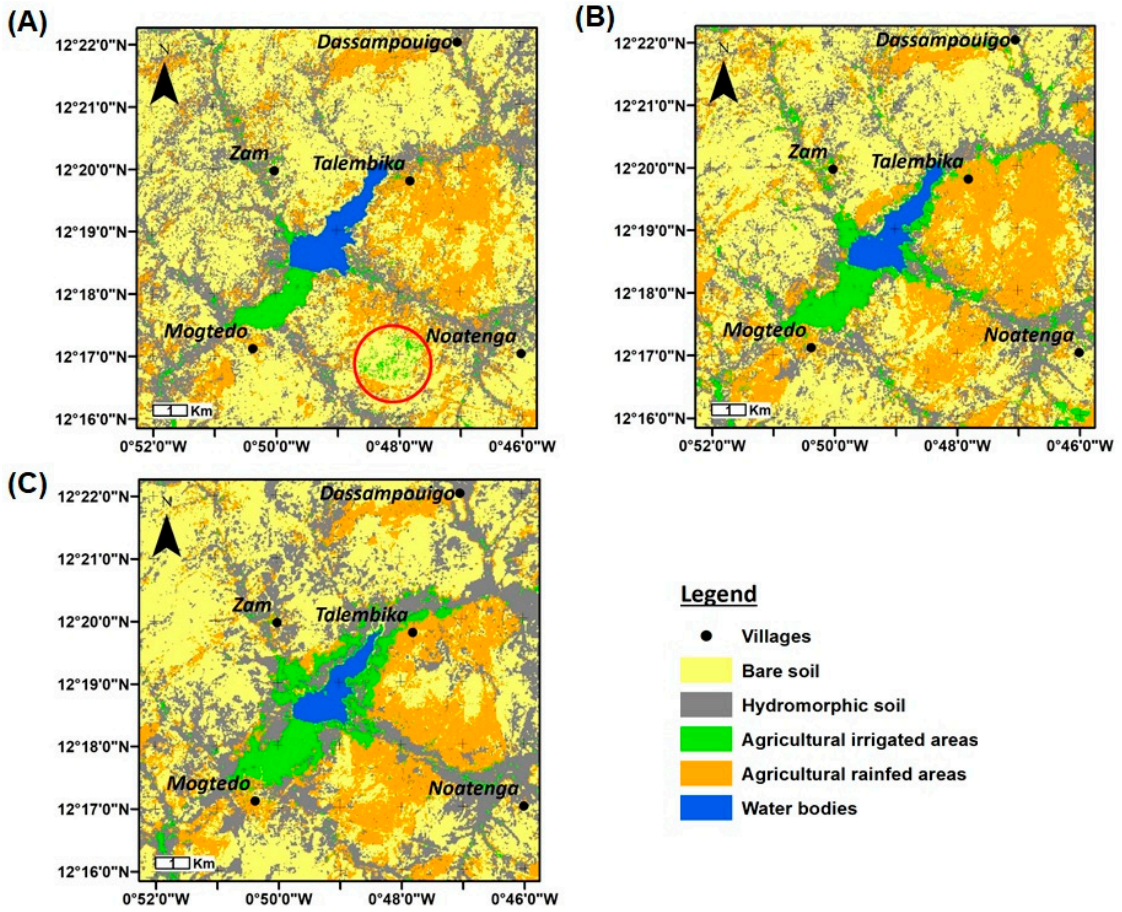

Figure 4. Initial classification of the different satellite images. (**A**) Landsat-5 TM image (15 February 1987); (**B**) Landsat-7 ETM+ image (11 February 2000); (**C**) Landsat-8 OLI image (27 January 2015).

4.2. Pixel Temporal Trajectory Analysis and Trajectory Corrections

Given the development of agricultural activities in the Mogtedo region and based on the field surveys and information provided by farmers and local authorities, it would be unlikely to see trajectories where the acreage of irrigated agricultural areas tended to be reduced over time. Examples of incorrect pixel trajectory are provided as follows:

- Transition from irrigated areas to rainfed areas: rainfed agriculture was practiced on the hillsides, while irrigated areas were found close to the water reservoir where flooding could occur during the rainy season.
- Transition from irrigated areas to bare soil: fallow was not an option in crop rotation in irrigated areas.
- Transition from irrigated areas to water bodies.

Table 4 shows the 125 unique pixel trajectories (initial and corrected) for the five LULC classes across the study region. For example, in case 5 in Table 4, the pixel was initially classified as bare soil (1) in 1987 and 2000, and then as water body (5) in 2015. The latter class attributed to that pixel being incorrect, it was corrected and bare soil was chosen for all three years.

Table 4. Unique pixel temporal trajectories for the different LULC classes and suggested correction.

N°	Initial Trajectory	Corrected Trajectory	N°	Initial Trajectory	Corrected Trajectory	No.	Initial Trajectory	Corrected Trajectory	No.	Initial Trajectory	Corrected Trajectory
1	1->1->1	1->1->1	41	2->4->1	1->1->1	81	4->2->1	1->1->1	121	5->5->1	5->5->2
2	1->1->2	1->1->1	42	2->4->2	2->2->2	82	4->2->2	2->2->2	122	5->5->2	5->5->2
3	1->1->3	1->1->3	43	2->4->3	4->4->4	83	4->2->3	4->4->4	123	5->5->3	5->5->2
4	1->1->4	1->1->4	44	2->4->4	4->4->4	84	4->2->4	4->4->4	124	5->5->4	5->5->2
5	1->1->5	1->1->1	45	2->4->5	5->5->5	85	4->2->5	5->5->5	125	5->5->5	5->5->5
6	1->2->1	1->1->1	46	2->5->1	1->1->1	86	4->3->1	1->1->1			
7	1->2->2	2->2->2	47	2->5->2	2->2->2	87	4->3->2	2->2->2			
8	1->2->3	1->1->3	48	2->5->3	2->2->3	88	4->3->3	4->3->3			
9	1->2->4	1->1->4	49	2->5->4	2->2->2	89	4->3->4	4->4->4			
10	1->2->5	2->2->2	50	2->5->5	5->5->5	90	4->3->5	5->5->5			
11	1->3->1	1->1->1	51	3->1->1	1->1->1	91	4->4->1	4->4->4			
12	1->3->2	2->2->2	52	3->1->2	2->2->2	92	4->4->2	4->4->4			
13	1->3->3	1->3->3	53	3->1->3	3->3->3	93	4->4->3	4->4->3			
14	1->3->4	1->1->4	54	3->1->4	1->1->4	94	4->4->4	4->4->4			
15	1->3->5	5->5->5	55	3->1->5	5->5->5	95	4->4->5	5->5->5			
16	1->4->1	1->1->1	56	3->2->1	1->1->1	96	4->5->1	1->1->1			
17	1->4->2	1->4->4	57	3->2->2	2->2->2	97	4->5->2	2->2->2			
18	1->4->3	1->4->4	58	3->2->3	3->3->3	98	4->5->3	4->4->4			
19	1->4->4	1->1->4	59	3->2->4	4->4->4	99	4->5->4	4->4->4			
20	1->4->5	5->5->5	60	3->2->4	5->5->5	100	4->5->5	5->5->5			
21	1->5->1	1->1->1	61	3->3->1	3->3->3	101	5->1->1	1->1->1			
22	1->5->2	2->2->2	62	3->3->2	3->3->3	102	5->1->2	5->2->2			
23	1->5->3	2->2->2	63	3->3->3	3->3->3	103	5->1->3	5->2->3			
24	1->5->4	1->4->4	64	3->3->4	3->3->3	104	5->1->4	1->1->4			
25	1->5->5	5->5->5	65	3->3->5	5->5->5	105	5->1->5	5->5->5			
26	2->1->1	1->1->1	66	3->4->1	1->1->1	106	5->2->1	5->2->2			
27	2->1->2	2->2->2	67	3->4->2	2->2->2	107	5->2->2	5->2->2			
28	2->1->3	1->1->3	68	3->4->3	3->3->3	108	5->2->3	5->2->3			
29	2->1->4	1->1->4	69	3->4->4	4->4->4	109	5->2->4	5->2->2			
30	2->1->5	5->5->5	70	3->4->5	5->5->5	110	5->2->5	5->5->5			
31	2->2->1	2->2->2	71	3->5->1	1->1->1	111	5->3->1	1->1->1			
32	2->2->2	2->2->2	72	3->5->2	2->2->2	112	5->3->2	5->2->2			
33	2->2->3	2->2->2	73	3->5->3	3->3->3	113	5->3->3	5->3->3			
34	2->2->4	2->2->2	74	3->5->4	4->4->4	114	5->3->4	4->4->4			
35	2->2->5	5->5->5	75	3->5->5	5->5->5	115	5->3->5	5->5->5			
36	2->3->1	1->1->1	76	4->1->1	1->1->1	116	5->4->1	1->1->1			
37	2->3->2	2->2->2	77	4->1->2	2->2->2	117	5->4->2	5->2->2			
38	2->3->3	3->3->3	78	4->1->3	1->1->3	118	5->4->3	5->3->3			
39	2->3->4	4->4->4	79	4->1->4	4->4->4	119	5->4->4	4->4->4			
40	2->3->5	5->5->5	80	4->1->5	5->5->5	120	5->4->5	5->5->5			

1: Bare soil; 2: Hydromorphic soil; 3: Agricultural irrigated areas; 4: Agricultural rainfed areas; 5: Water body.

4.3. Accuracy Assessment after Pixel Trajectory Corrections

The OA was improved after the corrections, particularly for the 1987 and 2000 images (Landsat 5 TM and Landsat 7 ETM+) (Table 5). The OA increased from 88.48% to 94.22% for the Landsat 5 TM image, and from 90.98% to 95.38% for the Landsat 7 ETM+ image. Similar improvements were also found for kappa coefficients (Table 5).

Table 5. Accuracy assessment after pixel trajectory corrections.

Images	Overall Accuracy (%)	Kappa Coefficient	Agreement*
Landsat-5 TM	94.22	0.92	Excellent
Landsat-7 ETM+	95.38	0.94	Excellent
Landsat-8 OLI	95.60	0.94	Excellent

*According to Landis and Koch [45] and Streiner and Norman [55].

Likewise, with regards to LULC classification, there was an improvement in the accuracy (Table 6). The user accuracy remained high and ranged from 89.09 to 100%. Confusions between classes were reduced in the majority of cases for all three images, except between rainfed areas and bare soils on the Landsat 5 TM image (confusion of 14.02%). Although the results were satisfactory, it is worth noting

that for features smaller than one Landsat pixel (for example, very small farms) or mixed-crop areas pixels, the distinction between classes can be difficult and would result in mixed-class pixels [12].

Table 6. Classification accuracy (expressed in %) after pixel trajectory corrections for each of the LULC classes in the Mogtedo region, Burkina Faso.

	Bare Soil	Hydromorphic Soil	Irrigated Areas	Rainfed Areas	Water Bodies	User Accuracy
			Landsat 5 TM			
Bare soil	**96.96**	5.78	0.52	14.02	0	91.78
Hydromorphic soil	0.89	**91.21**	0	0.46	0	96.03
Irrigated areas	0	1.26	**98.95**	0	0	98.69
Rainfed areas	2.15	1.51	0.52	**85.52**	0	93.81
Water bodies	0	0.25	0	0	**100**	99.6
			Landsat 7 ETM+			
Bare soil	**96.51**	4.43	1.4	4.73	0	95.87
Hydromorphic soil	0.89	**91.15**	3.33	0.46	0	91.15
Irrigated areas	0	1.3	**94.21**	0	0	99.08
Rainfed areas	2.6	2.6	1.05	**94.82**	0	92.42
Water bodies	0	0.52	0	0	**100**	99.19
			Landsat-8 OLI			
Bare soil	**94.44**	3.65	0	1.07	0	98.38
Hydromorphic soil	0.89	**91.67**	3.33	0.46	0	91.19
Irrigated areas	0	1.56	**95.96**	0.15	0	98.74
Rainfed areas	4.67	3.13	0.7	**98.32**	0	89.09
Water bodies	0	0	0	0	**100**	100

A visual analysis of all LULC classes in the Mogtedo region between 1987, 2000, and 2015 confirms the main results found before the image post-processing (pixel trajectory corrections); that is, increased proportions of irrigated areas around the reservoir and hydromorphic soils, and a decrease in water bodies (Figure 5).

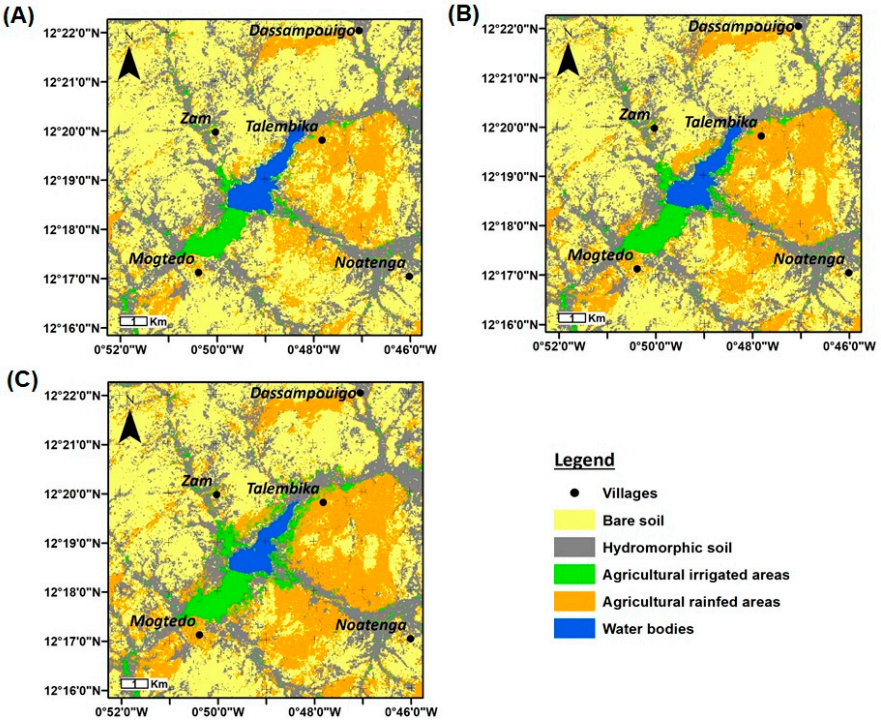

Figure 5. Classification of the different satellite images after pixel trajectory corrections. (**A**) Landsat-5 TM image (15 February 1987); (**B**) Landsat-7 ETM+ image (11 February 2000); (**C**) Landsat-8 OLI image (27 January 2015).

4.4. Changes of LULC Classes Between 1987 and 2015

The proportion of changes in LULC classes between the three time intervals 1987–2000, 2000–2015, and 1987–2015 are presented in Figure 6 and Tables S2 and S3. For a given LULC class, total, net, and swap changes were computed [49,50,53]. The total change is the sum of gross gain and loss in percentage of map. The net change corresponds to the difference between the gross gain and loss, and the swap change refers to the difference between the total and net changes. Between 1987 and 2000 irrigated and rainfed agricultural areas increased by 0.58% and 5.34%, respectively (percentage of net changes in Figure 6A). This reflects a dynamic within the agricultural sector linked to the settlement of new migrant farmers in the Mogtedo region. The increase in irrigated agricultural areas (+ 1.18%; Figure 6B) observed between 2000 and 2015 could be explained by the promotion of small-scale irrigation (officially launched in 2001 by the Government of Burkina Faso). During the three time intervals, the noticeable decreases were recorded for bare soils (Figure 6).

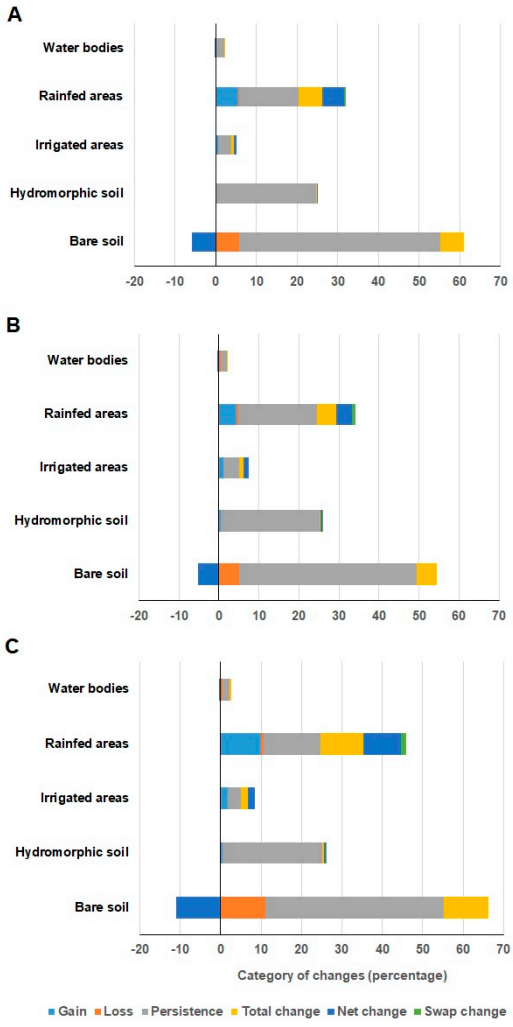

Figure 6. Quantity of LULC transition for three time intervals 1987–2000 (**A**); 2000–2015 (**B**); and 1987–2015 (**C**) across the Mogtedo region.

The speed and intensity of LULC changes between 1987 and 2015 are provided in Figures 7–9. The increase in irrigated agricultural areas between 1987 and 2000 occurred at the expense of wetlands (or water bodies) and rainfed agricultural areas (Figure 7). This change from wetlands to irrigated areas was located up the Mogtedo dam where farmers from surrounding villages (Zam and Talembika) settled gradually in this area to practice counter-season agriculture. The increase in agricultural areas (irrigated and rainfed) in the Mogtedo region can also be explained by the attractiveness of this

region for economic migrants since Mogtedo stands as the largest trading center in the region [30,56]. Crops such as rice and vegetables are produced predominantly for export to neighboring countries (Togo, Niger, and Ghana) [57,58], and can generate substantial incomes. Between 2000 and 2015, the increase in irrigated agricultural areas was detrimental to bare soils, in addition to rainfed agricultural land areas. With the boom in small-scale private irrigation and the pressure on existing agricultural lands, bare soils located near the water reservoir were progressively converted into irrigated areas. The 2000–2015 time interval was faster in LULC transformations (Figure 8). Between 1987–2000 and 2000–2015 the majority of LULC classes were active in terms of intensity of change (gain or loss) (Figure 9). Exceptions included hydromorphic soils.

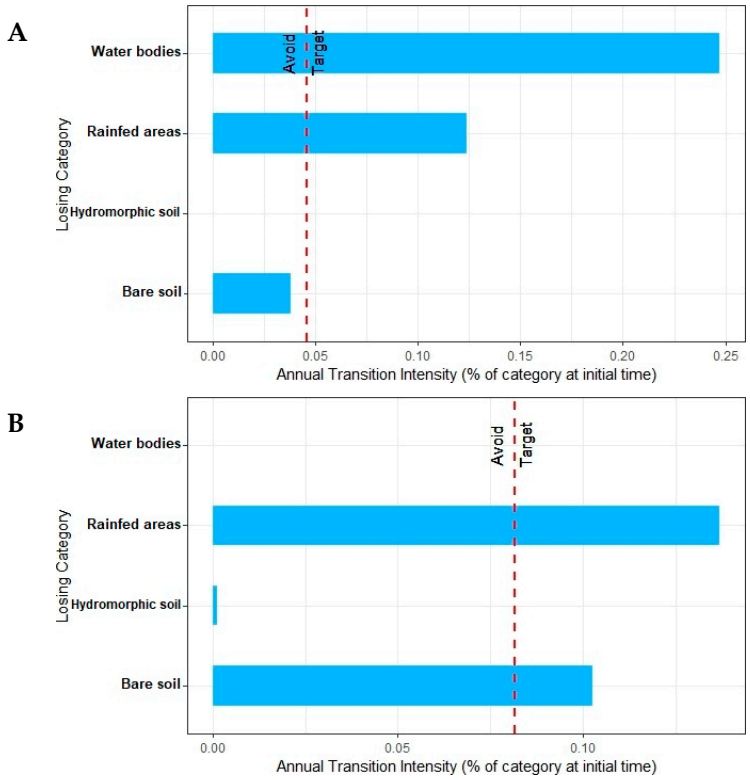

Figure 7. Annual transition intensity for gain of irrigated areas between 1987–2000 (**A**) and 2000–2015 (**B**) in the Mogtedo region.

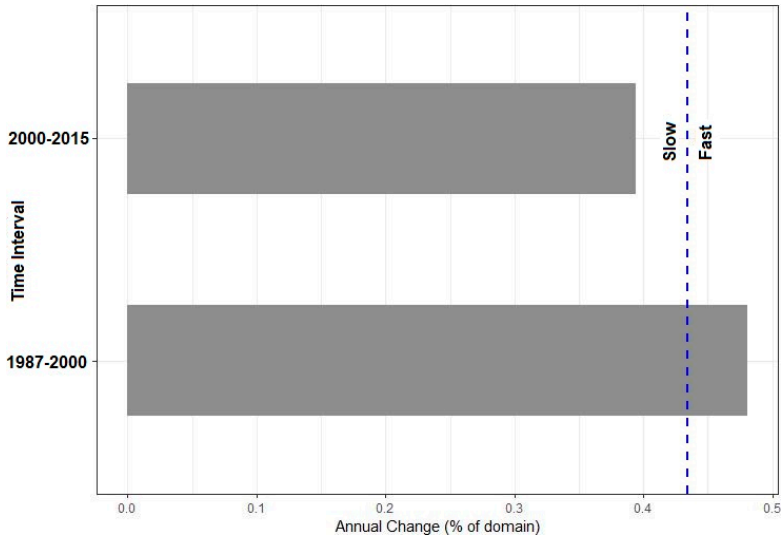

Figure 8. Time interval change intensity for the periods 1987–2000 and 2000–2015.

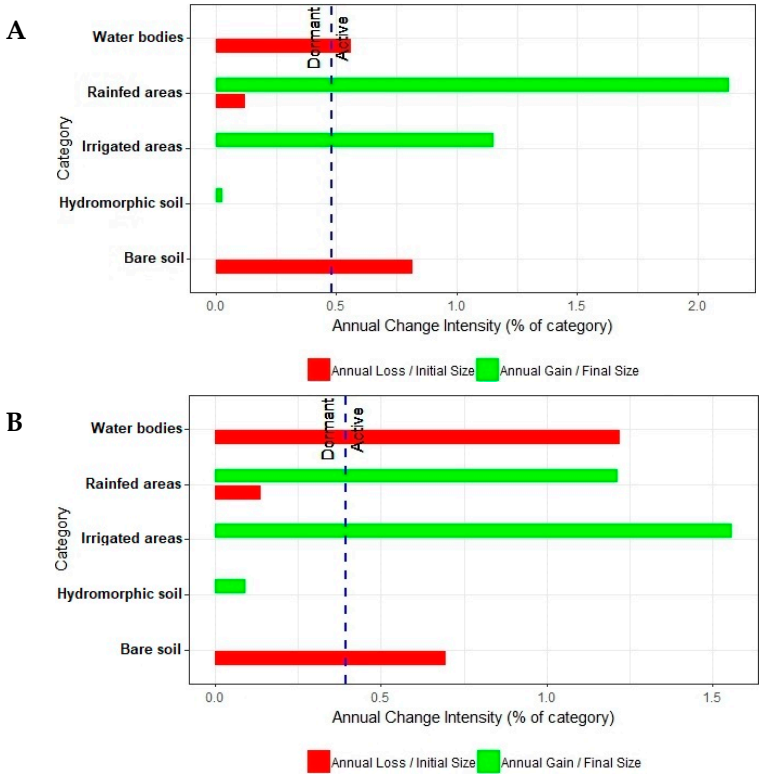

Figure 9. Annual change intensity for each of the LULC classes between the periods 1987–2000 (**A**) and 2000–2015 (**B**).

In terms of acreages, rainfed agricultural areas increased from 2,120 ha in 1987 to 3,455 ha in 2015 (Figure 10). This included 1,429 ha bare soils which were sown during this period. There was a shift of 93.51 ha from rainfed areas to irrigated areas during the same period. Between 1987 and 2015 irrigated areas increased from 470 ha to 722 ha (+53%) (Figure 10).

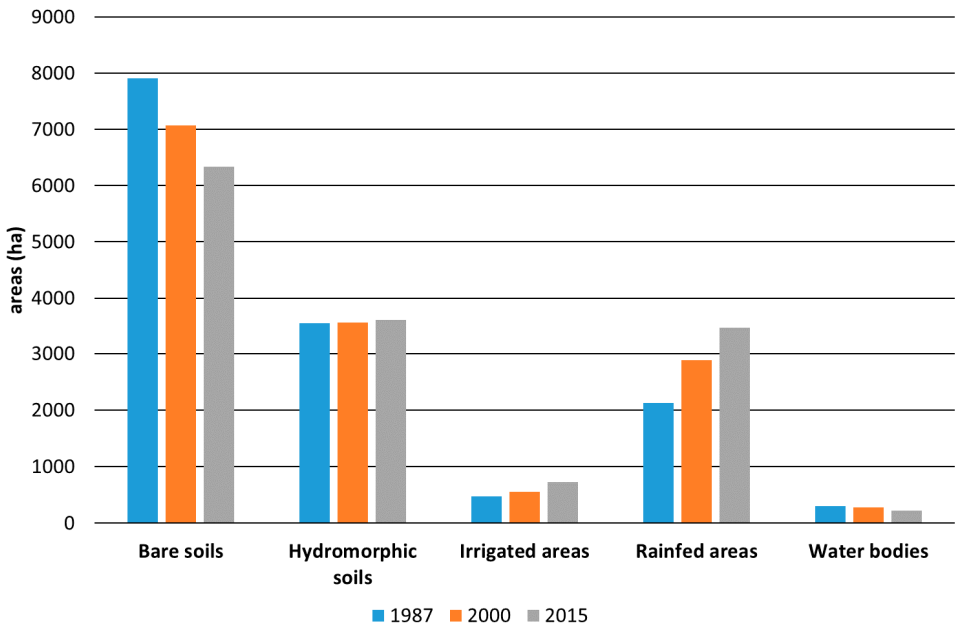

Figure 10. Acreages of LULC classes in 1987, 2000, and 2015 across the Mogtedo region, as determined using Landsat images (this study).

The decrease in areas of water bodies found in this study was in line with the conclusions of Guyon et al. [29], who denoted that the reservoir water volume decreased by ~33% between 1964 and 2014, mainly because of sedimentation. Indeed, the reservoir has been subject to increased silting since its building [28,59]. Between 1963 and 1991 the rate of silting was about 65,714 m^3 $year^{-1}$ [28] and 109,667 m^3 $year^{-1}$ between 1987 and 2002 [59]; that is, an increase of silting rate of 43,953 m^3 $year^{-1}$ between the two periods. There is also a gradual degradation of the dike and spillway (water erosion, seeps) despite the several rehabilitation actions [60].

There are few comprehensive available studies dealing with the census of irrigated agricultural areas in 1987 in Burkina Faso. One of the reliable source was [30] and was based on data collected during the reservoir building in 1967. Wellens [34] estimated the water consumption (irrigation, livestock farming, domestic use) at approximatively 3,500,000 m^3 $year^{-1}$ for the study region. Considering an estimated evaporation rate of 47% per year [29], the volume of water available would be of 3,700,000 m^3 $year^{-1}$, that is a satisfaction ratio of water requirements of 1.07.

Given the precarious balance that exists between water requirements and available water resources, if the increasing trend towards new irrigated farmland, coupled with the reduced storage capacity of the Mogtedo (under the effect of sedimentation), continues without any well-managed development plan, the reservoir would no longer meet the needs of its various users in future. According to Ibrahim [26] the outlook for climate change based on regional climate models projections (CCLM (COnsortium for Small scale MOdeling - Climate Limited-area Modelling), RACMO (Regional Atmospheric Climate MOdel), and RCA (Rossby Centre regional Atmospheric climate model)) for the period 2021–2050 shows a high risk of more variable climate conditions with marked decrease in rainfall and subsequent non-filling of the water reservoir at the end of the rainy season. Such climate conditions will worsen the precarious state of the reservoir water use.

The methodology used in this study addressed the challenge of building up historical spatial information database in data-scarce environments. It relies on first order or higher Markov chains [61–63], with the difference being the inclusion of rules based on field observations and expert knowledge. The methodology has been tested successfully in Burkina Faso for discriminating irrigated agricultural areas across the Kou [17] and Upper-Comoé watersheds [64]. The difference between the studies relies on the classification technique used (MLC in the former studies and SVM in this study). The results indicated an increase in irrigated areas by ~70% in 20 years for the Kou watershed, particularly between 2000 and 2009. For the Upper-Comoé watershed, the same change detection analysis showed that irrigated areas increased by more than 32% in 29 years (1986 to 2015).

In this study, the SVM classifier outperformed the MLC in two out of the three cases (1987 and 2000; Table 7); there was no difference in performance for the 2015 satellite image. Moreover, the SVM was used in land use classification analyses in Banfora, Burkina Faso (not shown), with similar performance compared to MLC (OA and kappa coefficient from the SVM equaled 81.83% and 0.78; respective values from the MLC being 77.83% and 0.73). Such results indicate that SVM would be a good choice for classifying satellite RS data when the number of training points is limited.

Table 7. Comparison between the Support Vector Machine (SVM) and Maximum Likelihood Classifier (MLC) for the classification of the 1987 and 2000 satellite images.

Year	Classifier	Overall Accuracy (%)	Kappa Coefficient
1987	MLC	86.76	0.82
	SVM	88.48	0.84
2000	MLC	89.64	0.86
	SVM	90.98	0.88

The method used in this study can be applied in different regions or countries with similar conditions and needs for better irrigation water management. The quantification of changes in LULC around the Mogtedo reservoir provided insightful information that can be used for decision-support

in short- and medium-term management plans. However, there are some limits to its application that need to be addressed. They include the number of LULC classes to be evaluated (several LULC classes make it uncertain the determination/correction of pixel trajectories) and the time period to be considered (the longer the period, the more difficult historical field data become ascertainable).

5. Conclusions

We quantified the changes in LULC around the Mogtedo water reservoir between 1987 and 2015 using Landsat imagery. Satellite images were classified using the SVM method, and post-processed based on and pixel trajectory analysis and correction to improve the classification results. The 2000–2015 period was faster in terms of LULC transformations compared to the 1987–2000 period. Changes in LULC classes were marked by an increase in irrigated agricultural areas between 1987 and 2000, at the expense of water bodies and rainfed agricultural areas. Between 2000 and 2015, the increase in irrigated agricultural areas occurred at the expense of rainfed agricultural areas and bare soils. With the irrigation water requirements estimated at 3,500,000 m^3 $year^{-1}$ and agricultural areas still expanding, such a decrease in irrigation water availability threatened the sustainability of agricultural activities in the Mogtedo region and could lead to more food insecurity and conflicts between the various stakeholders.

Supplementary Materials: The following are available online at http://www.mdpi.com/2072-4292/11/12/1442/s1.

Author Contributions: Conceptualization, F.T., J.W., and B.T.; Formal analysis, F.T.; Investigation, J.B. and J.C.; Methodology, F.T.; Supervision, B.T.; Writing—original draft, F.T.; Writing – review & editing, L.K., E.H., J.W., and B.T.

Acknowledgments: We are grateful to the Wallonie-Bruxelles International (WBI), the Association pour la Promotion de l'Emploi et de la Formation à l'Etranger (APEFE), and Institut Scientifique de Service Public (ISSeP) for their financial support. We also gratefully acknowledge the contribution of the farmers who participated in the interviews and generously provided information about their production systems. We thank the three anonymous reviewers for their constructive comments.

Conflicts of Interest: The authors declare no conflict of interest.

References

1. FAO. Country Fact Sheet on Food and Agriculture Policy Trends—Burkina Faso, April 2014. Available online: http://www.fao.org/docrep/field/009/i3760e/i3760e.pdf (accessed on 19 March 2019).
2. Paturel, J.E.; Boubacar, I.; L'Aour, A.; Mahé, G. Analyses de grilles pluviométriques et principaux traits des changements survenus au 20ème siècle en Afrique de l'Ouest et Centrale. *Hydrolog. Sci. J.* **2010**, *55*, 1281–1289. [CrossRef]
3. Paturel, J.E.; Servat, E.; Delattre, M.O.; Lubes-Niel, H. Analyse de séries pluviométriques de longue durée en Afrique de l'Ouest et Centrale non sahélienne dans un contexte de variabilité climatique/Analysis of rainfall long series in non-Sahelian West and Central Africa within a context of climate variability. *Hydrolog. Sci. J.* **1998**, *43*, 937–946. [CrossRef]
4. Ali, A.; Lebel, T. The Sahelian standardized rainfall index revisited. *Int. J. Climatol.* **2008**, *29*, 1705–1714. [CrossRef]
5. Benoît, E. Les changements climatiques: Vulnérabilité, impacts et adaptation dans le monde de la médecine traditionnelle au Burkina Faso. *VertigO—La revue Électronique en Sciences de L'environnement* **2008**, *8*, 1–13. [CrossRef]
6. Lebel, T.; Ali, A. Recent trends in the Central and Western Sahel rainfall regime (1990–2007). *J. Hydrol.* **2009**, *375*, 52–64. [CrossRef]
7. Ibrahim, B.; Karambiri, H.; Polcher, J.; Yacouba, H.; Ribstein, P. Changes in rainfall regime over Burkina Faso under the climate change conditions simulated by 5 regional climate models. *Clim. Dynam.* **2014**, *42*, 1363–1381. [CrossRef]
8. Yameogo, S.; Kienou, A. *Analysis of Public Expenditures in Support of Food and Agriculture Development in Burkina Faso, 2006–2010*; Technical Notes Series; MAFAP, FAO: Rome, Italy, 2013; Available online: http://www.fao.org/3/a-at461e.pdf (accessed on 19 March 2019).

9. Ministère de l'agriculture de l'hydraulique et des ressources halieutiques. *Politique Nationale de Développement Durable de L'agriculture Irriguée: Stratégie, Plan D'action, Plan D'investissement à L'horizon 2015*; Rapport Principal; MAHRH: Ouagadougou, Burkina Faso, 2006.
10. FAO. *Analyse des Dépenses Publiques en Soutien à L'agriculture et au Développement Rural au Burkina Faso, 2006–2013*; Programme de Suivi et Analyses des Politiques Agricoles et Alimentaires (SAPAA), Série de Notes Techniques; MAFAP, FAO: Rome, Italy, 2014; Available online: http://www.fao.org/3/a-i4513f.pdf (accessed on 19 March 2019).
11. Thenkabail, P.S.; Biradar, C.M.; Noojipady, P.; Dheeravath, V.; Li, Y.; Velpuri, M.; Gumma, M.; Gangalakunta, O.R.P.; Turral, H.; Cai, X.; et al. Global irrigated area map (GIAM), derived from remote sensing, for the end of the last millennium. *Int. J. Remote Sens.* **2009**, *30*, 3679–3733. [CrossRef]
12. Ozdogan, M.; Yang, Y.; Allez, G.; Cervantes, C. Remote sensing of irrigated agriculture: Opportunities and challenges. *Remote Sens.* **2010**, *2*, 2274–2304. [CrossRef]
13. Gumma, M.K.; Thenkabail, P.S.; Hideto, F.; Nelson, A.; Dheeravath, V.; Busia, D.; Rala, A. Mapping irrigated areas of Ghana using fusion of 30 m and 250 m resolution remote-sensing data. *Remote Sens.* **2011**, *3*, 816–835. [CrossRef]
14. Velpuri, N.M.; Thenkabail, P.S.; Gumma, M.K.; Biradar, C.B.; Noojipady, P.; Dheeravath, V.; Yuanjie, L. Influence of resolution in irrigated area mapping and area estimations. *Photogramm. Eng. Remote Sens.* **2009**, *75*, 1383–1395. [CrossRef]
15. Zoungrana, B.J.-B.; Conrad, C.; Amekudzi, L.K.; Thiel, M.; Da, E.D.; Forkuor, G.; Löw, F. Multi-Temporal Landsat Images and Ancillary Data for Land Use/Cover Change (LULCC) Detection in the Southwest of Burkina Faso, West Africa. *Remote Sens.* **2015**, *7*, 12076–12102. [CrossRef]
16. Knauer, K.; Gessner, U.; Fensholt, R.; Forkuor, G.; Kuenzer, C. Monitoring Agricultural Expansion in Burkina Faso over 14 Years with 30 m Resolution Time Series: The Role of Population Growth and Implications for the Environment. *Remote Sens.* **2017**, *9*, 132. [CrossRef]
17. Traoré, F.; Cornet, Y.; Denis, A.; Wellens, J.; Tychon, B. Monitoring the evolution of irrigated areas with Landsat images using backward and forward change detection analysis in the Kou watershed, Burkina Faso. *Geocarto Int.* **2013**, *28*, 733–752. [CrossRef]
18. Jin, N.; Tao, B.; Ren, W.; Feng, M.; Sun, R.; He, L.; Zhuang, W.; Yu, Q. Mapping irrigated and rainfed wheat areas using multi-temporal satellite data. *Remote Sens.* **2016**, *8*, 207. [CrossRef]
19. Basukala, A.K.; Oldenburg, C.; Schellberg, J.; Sultanov, M.; Dubovyk, O. Towards improved land use mapping of irrigated croplands: Performance assessment of different image classification algorithms and approaches. *Eur. J. Remote Sens.* **2017**, *50*, 187–201. [CrossRef]
20. Xiong, J.; Thenkabail, P.S.; Gumma, M.K.; Teluguntla, P.; Poehnelt, J.; Congalton, R.G.; Yadav, K.; Thau, D. Automated cropland mapping of continental Africa using Google Earth Engine cloud computing. *ISPRS J. Photogramm. Remote Sens.* **2017**, *126*, 225–244. [CrossRef]
21. Forkuor, G.; Hounkpatin, O.K.L.; Welp, G.; Thiel, M. High resolution mapping of soil properties using remote sensing variables in south-western Burkina Faso: A comparison of machine learning and multiple linear regression models. *PLoS ONE* **2017**, *12*, e0170478. [CrossRef]
22. Schug, F.; Okujeni, A.; Hauer, J.; Hostert, P.; Nielsen, J.Ø.; van der Linden, S. Mapping patterns of urban development in Ouagadougou, Burkina Faso, using machine learning regression modeling with bi-seasonal Landsat time series. *Remote Sens. Environ.* **2018**, *210*, 217–228. [CrossRef]
23. Société Africaine d'études et Conseils. *Plan Communal de Développement de Zam*; MATD: Ouagadougou, Burkina Faso, 2008; p. 104.
24. Sahelian Agency for Water Environment and Sanitation. *Plan Communal de Développement Sectoriel Approvisionnement en Eau Potable et Assainissement de la Commune de Mogtedo (Horizon 2010–2015)*; Gouvernorat du Plateau Central: Ziniaré, Burkina Faso, 2009; p. 57.
25. Ouédraogo, S. *Diagnostic Organisationnel Pour L'exploitation et la Gestion du Périmètre Irrigué de Mogtedo: Contrainte et Suggestions*; Rapport de fin de Cycle du Brevet de Technicien Supérieur; Centre Agricole Polyvalent de Matourkou: Matourkou, Burkina Faso, 2009.
26. Ibrahim, B. *Evaluation de la Prise en Compte de la Variabilité Climatique Dans la Gestion de la Retenue D'eau de Mogtedo au Burkina Faso*; WASCAL: Ouagadougou, Burkina Faso, 2016; p. 23.
27. Sally, H.; Lévite, H.; Cour, J. Local water management of small reservoirs: Lessons from two case studies in Burkina Faso. *Water Altern.* **2011**, *4*, 365–382.

28. Ndanga Kouali, G. *Compétition Entre Périmètres Irrigués Partageant la Même Ressource en Eau: Cas de Mogtedo et Talembika*; Mémoire de Master; 2iE: Ouagadougou, Burkina Faso, 2010.
29. Guyon, F.; Hallot, E.; De Thysebaert, D.; Diarra, B.G.; Roamba, J.; Zangré, B.V.C.A. Estimation de la sédimentation des retenues de Kierma, Wedbila et Mogtedo—Méthodologie et résultats obtenus. In Proceedings of the Atelier de capitalisation des résultats et Acquis du PADI, Ouagadougou, Burkina Faso, 14–15 November 2016.
30. Sally, H.; Keïta, A.; Ouattara, S. *Analyse Diagnostic et Performances de 5 Périmètres Irrigués Autour de Barrages au Burkina Faso*; Projet Management de l'Irrigation—Burkina Faso: Ouagadougou, Burkina Faso, 1997; p. 273.
31. Mas, J.F. Monitoring land-cover changes: A comparison of change detection techniques. *Int. J. Remote Sens.* **1999**, *20*, 139–152. [CrossRef]
32. Chander, G.; Markham, B.L. Revised Landsat-5 TM radiometric calibration procedures and postcalibration dynamic ranges. *IEEE Trans. Geosci. Remote Sens.* **2003**, *41*, 2674–2677. [CrossRef]
33. Chander, G.; Markham, B.L.; Helder, D.L. Summary of current radiometric calibration coefficients for Landsat MSS, TM, ETM+, and EO-1 ALI sensors. *Remote Sens. Environ.* **2009**, *113*, 893–903. [CrossRef]
34. Wellens, J. *Note Technique: Recensement Hydro-Agricole: Mogtedo—Mars 2012*; PADI-BF102: Ouagadougou, Burkina Faso, 2012; p. 7.
35. Richards, J.A.; Jia, X. *Remote Sensing Digital Image Analysis*, 4th ed.; Springer: Berlin/Heidelberg, Germany, 2006; p. 439. [CrossRef]
36. Ustuner, M.; Sanli, F.B.; Dixon, B. Application of support vector machines for landuse classification using high-resolution rapideye images: A sensitivity analysis. *Eur. J. Remote Sens.* **2015**, *48*, 403–422. [CrossRef]
37. Mountrakis, G.; Im, J.; Ogole, C. Support vector machines in remote sensing: A review. *ISPRS J. Photogramm. Remote Sens.* **2011**, *66*, 247–259. [CrossRef]
38. Vapnik, V.N. *The Nature of Statistical Learning Theory*; Springer: New York, NY, USA, 1995; p. 314. [CrossRef]
39. Gidudu, A.; Greg, H.; Marwala, T. Classification of Images Using Support Vector Machines. *arXiv* **2007**, arXiv:0709.3967.
40. Huang, C.; Davis, L.S.; Townshend, J.R.G. An assessment of support vector machines for land cover classification. *Int. J. Remote Sens.* **2002**, *23*, 725–749. [CrossRef]
41. Manandhar, R.; Odeh, I.O.A.; Ancev, T. Improving the accuracy of land use and land cover classification of Landsat data using post-classification enhancement. *Remote Sens.* **2009**, *1*, 330–344. [CrossRef]
42. Congalton, R.G.; Green, K. *Assessing the Accuracy of Remotely Sensed Data: Principles and Practices*, 2nd ed.; CRC/Taylor & Francis: Boca Raton, FL, USA, 2009; p. 200.
43. Banko, G. *A Review of Assessing the Accuracy of Classifications of Remotely Sensed Data and of Methods Including Remote Sensing Data in Forest Inventory*; International Institute for Applied Systems Analysis: Laxenburg, Austria, 1998; p. 42.
44. Foody, G.M. Status of land cover classification accuracy assessment. *Remote Sens. Environ.* **2002**, 185–201. [CrossRef]
45. Landis, J.R.; Koch, G.G. The measurement of observer agreement for categorical data. *Biometrics* **1977**, *33*, 159–174. [CrossRef]
46. Pontius, R.G.; Shusas, E.; McEachern, M. Detecting important categorical land changes while accounting for persistence. *Agr. Ecosyst. Environ.* **2004**, *101*, 251–268. [CrossRef]
47. Alo, C.A.; Pontius, R.G. Identifying systematic land-cover transitions using remote sensing and GIS: The fate of forests inside and outside protected areas of southwestern Ghana. *Environ. Plan. B* **2008**, *35*, 280–295. [CrossRef]
48. Zhou, P.; Huang, J.; Pontius, R.G., Jr.; Hong, H. Land classification and change intensity analysis in a coastal watershed of Southeast China. *Sensors* **2014**, *14*, 11640–11658. [CrossRef] [PubMed]
49. Diwediga, B.; Agodzo, S.; Wala, K.; Le, Q.B. Assessment of multifunctional landscapes dynamics in the mountainous basin of the Mo River (Togo, West Africa). *J. Geogr. Sci.* **2017**, *27*, 579–605. [CrossRef]
50. Koglo, Y.S.; Gaiser, T.; Agyare, W.A.; Sogbedji, J.M.; Kouami, K. Implications of some major human-induced activities on forest cover using extended change matrix quantity and intensity analysis based on historical Landsat data from the Kloto District, Togo. *Ecol. Indic.* **2019**, *96*, 628–634. [CrossRef]
51. Pontius, R.G.; Gao, Y.; Giner, N.M.; Kohyama, T.; Osaki, M.; Hirose, K. Design and Interpretation of Intensity Analysis Illustrated by Land Change in Central Kalimantan, Indonesia. *Land* **2013**, *2*, 351–369. [CrossRef]

52. Gao, Y.; Pontius, R.G.; Giner, N.M.; Kohyama, T.S.; Osaki, M.; Hirose, K. Land Change Analysis from 2000 to 2004 in Peatland of Central Kalimantan, Indonesia Using GIS and an Extended Transition Matrix. In *Tropical Peatland Ecosystems*; Osaki, M., Tsuji, N., Eds.; Springer: Tokyo, Japan, 2016; pp. 433–443. [CrossRef]
53. Aldwaik, S.Z.; Pontius, R.G. Intensity analysis to unify measurements of size and stationarity of land changes by interval, category, and transition. *Landsc. Urban Plan.* **2012**, *106*, 103–114. [CrossRef]
54. R Core Team. *R: A Language and Environment for Statistical Computing*; R Foundation for Statistical Computing: Vienna, Austria, 2016; Available online: https://www.R-project.org/. (accessed on 25 May 2019).
55. Streiner, D.L.; Norman, G.R. *Health Measurement Scales: A Practical Guide to Their Development and Use*, 3rd ed.; Oxford University Press: New York, NY, USA, 2003; p. 296.
56. Institut National de la Statistique et de la Démographie (INSD). *Projections Démographiques des Communes du Burkina Faso de 2007 à 2020*; Institut National de la Statistique et de la Démographie (INSD): Ouagadougou, Burkina Faso, 2017; pp. 1488–1492, 1498–1502. Available online: http://www.insd.bf/n/contenu/autres_publications/Projection_com_Burkina_2007_2020.pdf (accessed on 19 March 2019).
57. Sanfo, S. Politiques Publiques Agricoles et Lutte Contre la Pauvreté au Burkina Faso: Le cas de la Région du Plateau Central. Ph.D. Thesis, Université Paris 1 Panthéon-Sorbonne, Paris, France, 2010.
58. INSD. *Analyse des Résultats de L'enquête Burkinabé sur les Conditions de vie Des Ménages—Rapport Final*; Institut National de la Statistique et de la Démographie: Ouagadougou, Burkina Faso, 2003; p. 270.
59. Padonou, M.N.; Sarr, P. Contribution de la Télédétection et du Système d'Information Géographique à l'amélioration de la gestion des eaux de surface dans un bassin versant: Cas du barrage de Mogtedo au Burkina Faso. In Proceedings of the Journées d'Animation Scientique (JAS'09) de l'AUF, Alger, Algérie, 8–11 Novembre 2009; p. 7.
60. Tao, A. Mogtedo: Le barrage se meurt, la ville aussi. *FENOP Info* **2016**, *24*, 2–3.
61. Parzen, E. *Stochastic Processes*; Holden-Day: San Francisco, CA, USA, 1964; p. 324.
62. Bell, E.J.; Hinojosa, R.C. Markov analysis of land use change: Continuous time and stationary processes. *Soc. Econ. Plan. Sci.* **1977**, *11*, 13–17. [CrossRef]
63. Petit, C.; Scudder, T.; Lambin, E. Quantifying processes of land-cover change by remote sensing: Resettlement and rapid land-cover changes in south-eastern Zambia. *Int. J. Remote Sens.* **2001**, *22*, 3435–3456. [CrossRef]
64. Traoré, F.; Paré, K.; Walbeogo, R.; Wellens, J.; Tychon, B. *Estimation de L'évolution des Superficies Agricoles Irriguées du Bassin de la Haute-Comoé—Application D'une Méthode de Détection de Changements Amont et Aval*; Rapport PADI (Programme d'Appui au Développement de l'Irrigation); PADI: Ouagadougou, Burkina Faso, 2016.